Comptes Rendus Mécanique, Volume 347, Issue 9, September 2019, pp. 615-625
DOI: 10.1016/j.crme.2019.07.003

Experimental and numerical study on the effect of silica filler on tensile strength of 3D printed particulate nanocomposite

Muhammad Asif[1,2], Maziar Ramezani[1,*], Kamran Ahmed Khan[4], Muhammad Ali Khan[5], Kean Chin Aw[3]

[1]*Department of Mechanical Engineering, Auckland University of Technology, Auckland, New Zealand*

[2]*Department of Engineering Sciences, National University of Science and Technology, Karachi, Pakistan*

[3] *Department of Mechanical Engineering, University of Auckland, Auckland ,New Zealand*

[4]*Aerospace Engineering Department, Khalifa University, Abu Dhabi, UAE*

[5]*School of Aerospace, Transport and Manufacturing, Cranfield University, UK*

[*] Corresponding author, Email: maziar.ramezani@aut.ac.nz

Abstract

Polymers are commonly found to have low mechanical properties e.g. low stiffness and low strength. To improve the mechanical properties of polymers, various types of fillers are added. These fillers can be either micro or nano sized, however nano sized fillers are found to have more profound effect on improving the mechanical properties compared to micro sized fillers. In this research, we have analysed the mechanical behaviour of the silica reinforced nanocomposites printed by using a new 5 axis photopolymer extrusion 3D printing technique. The printer has 3 translational axis and 2 rotational axis which enables it to print free standing objects. Since this is a new technique and in order to characterise the mechanical properties of the nanocomposites manufactured using this new technique, we carried out experimental and numerical analyses. We added nano sized silica filler to enhance the properties of 3D printed photopolymer. Different concentrations of the filler were added and their effects on mechanical properties were studied by conducting uniaxial tensile tests. We observed improvement in mechanical properties by the addition of nano sized filler. In order to observe the tensile strength, dog-bone samples using new photopolymer extrusion printing were prepared. A viscoelastic model was developed and stress relaxation tests were conducted on photopolymer in order to calibrate the viscoelastic parameters. The developed computational model of nano reinforced polymer composite takes into account the nanostructure and dispersion of nanoparticles. Hyper and viscoelastic phenomena was employed to validate and analyse the stress-strain relationship of 8%, 9% and 10% filler concentrations. In order to represent the nanostructure, a 3D representative volume element (RVE) was utilized and subsequent simulations were ran in commercial finite element package ABAQUS. Results acquired in this study could lead to better understanding of the mechanical characterisation of the nanoparticle reinforced composite, manufactured using the new photopolymer extrusion 5-axis 3D printing technique.

Keywords: *3D printing; Hyperelastic; Photopolymer Extrusion; Viscoelastic.*

1. Introduction

The most common technique to enhance the properties of polymers is the adding of reinforcements for example nanoparticles or fibres. Several composites have been manufactured by adding micro sized reinforcements in the past twenty years [1-3]. In the past two decades, nano sized reinforcements have attracted a significant interest from scientific and industrial sectors. In fact, the nano sized reinforced composites have proven to show better mechanical behaviour when compared with conventional ones [4, 5]. Especially, significant amount of interest has been dedicated to bi-phase or multiphase systems in which inorganic nano fillers are added to the polymer. These nanometric fillers produce large surface area if homogenously distributed in the matrix; thus, these systems can potentially enhance the interfacial interaction between matrix and filler resulting in an improved mechanical properties of the material [6]. Researchers have reported considerable amount of enhancement in mechanical and tribological properties even at very low volume fractions [7]. Especially, some researchers have reported that ceramic and nano sized silica particles can prominently enhance bulk polymers' mechanical properties [7-9].

Finite Element Modelling (FEM) has been successfully implemented by some researchers to model the composites being reinforced with nanometric fillers. For instance, Liu and Chen [10] studied the possibility of applying FEM to composites reinforced with carbon nanotube using representative volume element (RVE). Other numerical techniques such as 3D FEM and 2D nano scale FEM were also used by other researchers to model the mechanical behaviour of nanocomposite materials [11-13]. It can be noted that such FEM based models are commonly executed by using representative volume elements, thus making the assumption that the nanocomposite microstructure can be replicated by gathering large quantity of these elements. An RVE normally has one or more nanofiller(s) which is surrounded by resin, and adequate loads or boundary conditions are applied to predict the effect of the surrounding materials. It is considered as a building block to accumulate the composite. Until now, majority of the studies focused on linear elastic properties and yielding predictions for the elastic toughness of the nanocomposites with respect to filler concentration, filler properties and in some cases filler orientation.

Zhang et al. [14] utilized the RVE technique to analyse the mechanical behaviour with particular attention to the damage mechanisms of SiCp reinforced Al composites using experiments and FEM. They developed a 3D microstructure FEM model predicting elasto-plastic behaviour and breakage behaviour of 7% volume fraction of SiCp reinforced Al

composite. Hua et al. [15] studied the mechanical behaviour of the dental composite resin reinforced with titanium oxide nanoparticles using a 3D nanoscale RVE. They characterised the effect of nano filler concentration, geometrical aspect, toughness and interphase zone among the matrix material and nano filler on bulk properties of the composite. Hua et al. [16] used nanoscale RVE to study interphase property and geometry effect on the mechanical behaviour of the silica-epoxy resin nanocomposite. They found that interphase modulus and interfacial bonding conditions have notable effect on effective stiffness of nanocomposites.

Three dimension (3D) printing commonly known as additive manufacturing follows the principle of laying down successive layers of material (sheet material, powder or liquid) on top of each other by detecting the data from CAD file [17, 18]. There are different 3D printers which are used to manufacture polymers, e.g. Stereolithogrpahy (SLA), Fused Deposition Modelling (FDM), UV assisted 3D Printing (UV3DP), etc. Micro and nano filler are added to enhance the properties of the polymers manufactured using these techniques. We have developed a novel photopolymer extrusion (PPE) 3D printing technique which uses 5-axis and is the combination of UV3DP and FDM techniques. This technique has three translational axes and 2 rotational axes. Photopolymer extrusion combined with two rotational axes on the extrusion unit provides the possibility of printing complex free from and free standing structures more easily. A peristaltic pump is used to accurately handle the quantity of material deposited. As discussed above, polymers exhibit weak mechanical properties, so we have added nano silica filler to enhance the mechanical properties of the nanocomposites manufactured using this technique. As this is a relatively new technique, there is a need to conduct experimental and numerical analyses to explore the mechanical strength and viscoelasticity of the nanocomposites printed.

A nanoscale RVE is used to predict the mechanical behaviour of fumed silica reinforced 3D printed particulate nanocomposite, different concentrations of the filler were added and dogbone samples were printed. Stress relaxation tests were conducted on the polymer to characterise the viscoelastic properties and tensile tests were conducted on each concentration to observe the tensile strength and strain to failure. Multi-scale material modelling platform DIGIMAT [19] was used to develop the RVE to represent the nanostructure of the composite, subsequent simulations were conducted in the commercial finite element software ABAQUS to validate the behaviour of the nanocomposite after importing the user defined python script as input.

2. Experimental Procedure

2.1 Photopolymer Extrusion (PPE) 3D Printer

Figure 1 shows the novel (PPE) 5-axis 3D printing machine. Figure 2 shows close up view of the new printer outlining the 5 axes and extrusion unit with 2 UV lasers on either side. The whole PPE 5-axes system consists of two UV laser diodes used to cure the photopolymer, peristaltic pump and nozzle which serves as an extrusion system and build platform consisting of conventional axes (X, Y and Z) along with two rotational axes (A & B).

This PPE 5-Axis 3D printer has FDM style extrusion system. Extruder unit is used to deposit the photopolymer resin. UV lasers mounted on each side of the printing nozzle cures the photopolymer soon after it leaves the nozzle [20].

2.2 Composition of Photopolymer Resin

The photopolymer resin used in this study (UV Dome 58), is supplied by Whitehall Technical Services Ltd, Auckland, New Zealand. It is an epoxy urethane in which fumed silica was utilized as a filler. As depicted in Figure 3, the filler used have a spherical shape having approximate size of between 25 to 30 nm. Fumed silica particles have the tendency to form agglomeration. The size of the agglomerates increases with the increase in particle loading. The photopolymer resin is curable with UV exposure at a wavelength of 405 nm.

In order to investigate the effect of filler on tensile strength of printed parts, specimens with varying concentrations of fumed silica (by weight) were composed by mixing it into the photopolymer. In order for the specimens to have same ageing, blends were composed the same day and the entire blends composition process was carried out inside a photolithography room. A 100 g of blend was prepared for every concentration, for example for 4% by weight of filler, 96 g of the photopolymer was mixed with 4 g of fumed silica filler. A thin spatula was used to manually stir the mixture for 5-10 minutes, after this the blend was mixed with an ultrasonic homogeniser. An ultrasonic homogeniser from Sonics and Materials Inc [21] was used for 2 minute at ultrasound frequency of 20 kHz and intensity of 130 W. In the end, to reduce air bubbles, specimens were vacuumed for 45 min at 65 $^{\circ}$C.

2.3 Adequate Material Viscosity for Printing

For well-ordered extrusion, the viscosity of the material has to be in an adequate range. Low viscosity is likely to cause the material to expand due to gravitational factor prior to the curing by the UV laser, high viscosity causes difficulties to deposit the material through the extruder unit. Therefore, the viscosities of the photopolymer blends were carefully calculated of the filler concentrations mentioned in Table 1 using a rheometer and their capability to print reliably was observed. In order to accurately measure the viscosity of the resin with the concentrations used, a 64 gauge spindle was used. For each sample, the revolution speed was adjusted to achieve a torque close to the midpoint (50%) of the sensor range. The rheometer then calculated the viscosity value based on the spindle, speed and measured torque.

As depicted in Table 1, substantial growth in the dynamic viscosity is detected with respect to increase in proportion of filler. Filler concentrations up to 6% have low viscosity and an abrupt increase in viscosity was seen with filler concentrations higher than 9%. A small scale of filler concentrations of 8%, 9% and 10% (compatible with dynamic viscosities from of 15000 cP to 25000 cP) with the extrusion nozzle of 21 gauge (0.5 mm) was found to be the appropriate range to have smooth printing.

2.4 Tensile Test

In order to observe the tensile strength of the parts printed, dog-bone specimens according to ASTM D638 standard type V (Figure 4) were printed (Figure 5) and tensile tests were conducted on each specimen to observe the tensile strength and strain to failure. Table 2 shows the process parameters used to print the samples, including the values used for layer heights and printing speed. Table 3 shows the mechanical properties of 8%, 9% and 10% filler concentrations. Each test set has been repeated three times and the average values are reported in Table 3.

As discussed in section 1, fillers are employed to enhance the mechanical properties of the polymers. However, there are certain characteristics on which the overall strength of the nanocomposite rely, e.g. matrix-particle interfacial adhesion, particle size and particle loading [22] . As it is generally understood that adding fillers might increase the mechanical properties of the nanocomposite, but stresses sometimes do not behave as it is expected [23]. Particle size plays a very important role in increasing the strength of the composite. Dittanet and Pearson [23] studied the effects of different particle sizes on tensile strength of the composite by increasing the volume fraction and concluded that nano sized particles increase

the tensile strength with increasing volume fraction. This is true as smaller particles have larger surface area providing more enhanced matrix-particle interfacial adhesion, which results in effective transfer of the stress from the matrix to particles. Increasing filler content increases the diameter of the filler and thereby decreasing the surface area which sometimes results in poor matrix-particle interfacial adhesion, and as a result, the nanoparticles cannot withstand majority of the externally applied force. Therefore, the mechanical properties of the composite will be similar as that of neat resin.

As shown in Table 3, tensile strength of sample with 8% filler concentration is higher than that of 9% and 10%; this is caused by better interfacial adhesion because at lower filler concentration nanoparticles have larger surface area which gives rise to better bond between matrix and nanoparticles. Tensile strength of 10% filler concentration is close to 9% but lower than 8% because higher filler content increases the diameter and decreases the surface area which results in weak interfacial adhesion leading to weak mechanical properties. Figure 6 shows the stress strain curves of the 8%, 9% and 10% filler concentrations, it can been seen that increasing volume fraction made the samples less elastic as strain at break of both 9% and 10% filler concentrations is smaller compared to 8% filler concentration.

3. Finite Element Simulations Procedure

3.1 Constitutive Equations

The experimental stress stain data of polymer (UV Dome 58) was used to calibrate an isotropic hyperelastic strain energy density function (SEDF) in ABAQUS in order to obtain the material constants to be used in FE simulations. After performing the curve fitting procedure in ABAQUS, out of various SEDF available, Yeoh's function captured the behaviour of the photopolymer more accurately as shown in Figure 7. Yeoh's model in the form of SEDF can be written as

$$W = \sum_{i=1}^{3} C_{i0}(\bar{\mathrm{I}}_1 - 3)^i + \sum_{i=1}^{N} \frac{1}{D_i}(J-1)^{2i} \quad (1)$$

where $J = \det(F)$ and F is considered as deformation gradient. The term $\bar{\mathrm{I}}_1$ is the first invariant of the left Cauchy-Green strain tensor B. ABAQUS employs linear least square fitting in order to calibrate the material constants. The calibrated material constants of the Yeoh's function are shown in Table 4.

3.2 Stress Relaxation Test

ABAQUS uses Prony series in order to obtain the coefficients of the viscoelastic material as shown in equations 2 and 3. To calibrate the Prony series coefficients in ABAQUS stress relaxation test was conducted at room temperature, sample was subjected to constant strain of 6% applied at the rate of 3 mm/min. Curve fitting procedure was carried out as shown in Figure 8, it is quite evident from Figure 8 that the normalized shear moduli obtained from ABAQUS are in good agreement with the experimental stress relaxation data. Table 5 shows the Prony series coefficients obtained by curve fitting procedure.

$$g_R(t) = 1 - \sum_{i=1}^{N} g_i^{-p}\left(1 - e^{\frac{-t}{\tau_i^G}}\right) \quad (2)$$

3.3 Finite Element Modelling

The nanostructure of silica reinforced photopolymer matrix nanocomposite is shown by a 3D RVE (220 nm each side) for 8%, 9% and 10% filler concentrations as shown in Figure 9 (a, b & c) respectively. 30 similar spherical silica nanoparticles are randomly dispersed in the matrix. Random sequential adsorption algorithm [24] is used to generate nanoparticle centres, in which probability of finding a nanoparticle at a given position is same in all directions. Nanoparticle diameter is dependent on the volume fraction and aspect ratio. Aspect ratio of 1 is chosen for all filler concentrations. As the silica nanoparticles have the diameter of around 30 nm shown in Figure 3, same is used for 8% filler concentration, the diameter increases with an increase in volume fraction. Elastic modulus of fumed silica nanoparticles was taken as E_p= 70 GPa and Poisson's ratio as υ_p= 0.3. For the properties of resin matrix epoxy urethane, calibrated Yeoh's hyperelastic material constants and Prony series coefficients were used as discussed in sections 4.1 and 4.2. Both phases are meshed with quadratic tetrahedron elements (C3D10M) with initial seed size of 11 nm as shown in Figure 10. In order to extend the RVE periodically periodic boundary conditions implemented from a user defined python script and were applied in all directions, i.e. observing the interlinkage among the RVE with its reflecting images. Displacement vector $\boldsymbol{u}$ was used to express the periodic boundary conditions, which relates the displacement among the opposed ends rendering to

$$\boldsymbol{u}(x, y, 0) - \boldsymbol{u_z} = \boldsymbol{u}(x, y, L)$$

$$\boldsymbol{u}(x, 0, z) - \boldsymbol{u_y} = \boldsymbol{u}(x, L, z)$$

$$\boldsymbol{u}(0, y, z) - \boldsymbol{u_x} = \boldsymbol{u}(L, y, z)$$

in which *L* corresponds to the RVE length and *x*, *y*, and *z* are coordinate axes and $\boldsymbol{u_x}$, $\boldsymbol{u_y}$ and $\boldsymbol{u_z}$ **is** dependent on the load applied to the RVE. A strain equal to the strain at break observed during uniaxial tensile test for each concentration was applied to the model in x-direction.

3.4 FE simulations and model verification

A nanoscale RVE reinforced by silica filler with different concentrations was validated in this study, FE simulations were ran on RVE composed of randomly dispersed nanoparticles with proper boundary conditions as discussed in section 3.3 and results were compared with experiments. Many researchers have validated the hyperelastic models with experimental data [25-28] using different FE packages. In order to validate the proposed model Yeoh's hyperelastic coefficients and Prony series coefficients were applied to the FE simulations of samples with filler concentrations of 8%, 9% and 10% and the results were compared with the tensile tests.

Figures 12, 14 & 16 show the contour plots of the 8%, 9% and 10% filler concentrations respectively. Figures 12 (a), 14 (a) & 16 (a) show the reaction forces of the respective filler concentrations, stress was obtained by dividing the area of RVE with reaction force. Figures 12 (b), 14 (b) & 16 (b) show the displacement of the respective filler concentration, strain was obtained by dividing the length of the RVE with displacement. Comparisons of the output obtained from the experiments and the FE model are depicted in Figures 11, 13 & 15. It is observed that the FE simulation with hyper and viscoelastic model using Yeoh's SEDF has good agreement with the experimental stress-strain curves of samples printed with 8%, 9% and 10% filler concentrations.

4. Conclusion

In this paper, mechanical properties of samples printed with a new 5-axis PPE printer have been studied. As this is a new technique and the mechanical behaviour of the samples printed is yet to be explored, we have successfully carried out experimental and numerical analysis on this new technique. Nano silica filler is used as reinforcement to enhance the mechanical properties of the photopolymer. Different concentration of fumed silica filler have been added and its effect on mechanical properties have been analysed. A significant improvement in the tensile strength of the photopolymer is observed; for example tensile strength after the addition of 8%, 9% and 10% silica filler is 1.87, 1.48 and 1.57 times the tensile strength of

the pure photopolymer respectively. Although not demonstrated in this paper, but the new PPE printer is capable of printing free form and self-supported structures with its 5-axis printing capability. A finite element model using hyper and viscoelastic phenomenon have been developed and successfully corroborated with the experimental results. Multi-scale material modelling platform DIGIMAT was used to develop the RVE to represent the nanostructure of the nanocomposite, silica nanoparticles were randomly dispersed and proper boundary conditions were applied. Properties of the matrix was represented by Yeoh's material constant and Prony series coefficients. FE simulations were conducted using ABAQUS after importing the user defined python script. The developed FE model based on hyper and viscoelastic phenomena successfully captured the behaviour of nano silica reinforced photopolymer composite manufactured using a new 5-axis PPE printer. By employing the combination of hyperelasticity and viscoelasticity the model is found to have good agreement with experimental stress-strain relationship of 8%, 9% and 10% filler concentrations.

References

1. Zhang, Q., M. Tian, Y. Wu, G. Lin and L. Zhang, *Effect of particle size on the properties of Mg(OH)2-filled rubber composites.* Journal of Applied Polymer Science, 2004. **94**(6): p. 2341-2346.
2. Lazzeri, A., Y.S. Thio and R.E. Cohen, *Volume strain measurements on CACO3/polypropylene particulate composites: The effect of particle size.* Journal of Applied Polymer Science, 2004. **91**(2): p. 925-935.
3. Nakamura, Y., M. Yamaguchi, M. Okubo and T. Matsumoto, *Effect of particle size on mechanical properties of epoxy resin filled with angular-shaped silica.* Journal of Applied Polymer Science, 1992. **44**(1): p. 151-158.
4. Ling Ji, X., J. Kai Jing, W. Jiang and B. Zheng Jiang, *Tensile modulus of polymer nanocomposites*. Vol. 42. 2002. 983-993.
5. Mishra, S., S.H. Sonawane and R.P. Singh, *Studies on characterization of nano CaCO3 prepared by the in situ deposition technique and its application in PP-nano CaCO3 composites.* Journal of Polymer Science Part B: Polymer Physics, 2005. **43**(1): p. 107-113.
6. Schmidt, D., D. Shah and E.P. Giannelis, *New advances in polymer/layered silicate nanocomposites.* Current Opinion in Solid State and Materials Science, 2002. **6**(3): p. 205-212.
7. Wetzel, B., F. Haupert and M.Q. Zhang, *Epoxy nanocomposites with high mechanical and tribological performance.* Composites Science and Technology, 2003. **63**(14): p. 2055-2067.
8. Wang, H., Y. Bai, S. Liu, J. Wu and C.P. Wong, *Combined effects of silica filler and its interface in epoxy resin.* Acta Materialia, 2002. **50**(17): p. 4369-4377.
9. Cannillo, V., F. Bondioli, L. Lusvarghi, M. Monia, M. Avella, M. Errico and M. Malinconico, *Modeling of ceramic particles filled polymer–matrix nanocomposites*. Vol. 66. 2006. 1030-1037.

10. Liu, Y.J. and X.L. Chen, *Evaluations of the effective material properties of carbon nanotube-based composites using a nanoscale representative volume element.* Mechanics of Materials, 2003. **35**(1): p. 69-81.
11. Katti, D.R., K.S. Katti, J.M. Sopp and M. Sarikaya, *3D finite element modeling of mechanical response in nacre-based hybrid nanocomposites.* Computational and Theoretical Polymer Science, 2001. **11**(5): p. 397-404.
12. Wang, X.Y. and X. Wang, *Numerical simulation for bending modulus of carbon nanotubes and some explanations for experiment.* Composites Part B: Engineering, 2004. **35**(2): p. 79-86.
13. Wang, Y., C. Sun, X. Sun, J. Hinkley, G.M. Odegard and T.S. Gates, *2-D nano-scale finite element analysis of a polymer field.* Composites Science and Technology, 2003. **63**(11): p. 1581-1590.
14. Zhang, J., Q. Ouyang, Q. Guo, Z. Li, G. Fan, Y. Su, L. Jiang, E.J. Lavernia, J.M. Schoenung and D. Zhang, *3D Microstructure-based finite element modeling of deformation and fracture of SiCp/Al composites.* Composites Science and Technology, 2016. **123**: p. 1-9.
15. Hua, Y., L. Gu and H. Watanabe, *Micromechanical analysis of nanoparticle-reinforced dental composites.* International Journal of Engineering Science, 2013. **69**: p. 69-76.
16. Hua, Y., L. Gu, S. Premaraj and X. Zhang, *Role of Interphase in the Mechanical Behavior of Silica/Epoxy Resin Nanocomposites.* Materials, 2015. **8**(6): p. 3519.
17. Kaye, R., T. Goldstein, D. Zeltsman, D.A. Grande and L.P. Smith, *Three dimensional printing: A review on the utility within medicine and otolaryngology.* Int J Pediatr Otorhinolaryngol, 2016. **89**: p. 145-8.
18. Rengier, F., A. Mehndiratta, H. von Tengg-Kobligk, C.M. Zechmann, R. Unterhinninghofen, H.U. Kauczor and F.L. Giesel, *3D printing based on imaging data: review of medical applications.* Int J Comput Assist Radiol Surg, 2010. **5**(4): p. 335-41.
19. *Digimat - muli-scale material modelling platform* Available from: https://www.e-xstream.com/products/digimat/about-digimat.
20. Asif, M., J.H. Lee, M.J. Lin-Yip, S. Chiang, A. Levaslot, T. Giffney, M. Ramezani and K.C. Aw, *A new photopolymer extrusion 5-axis 3D printer.* Additive Manufacturing, 2018. **23**: p. 355-361.
21. *Sonics and Materials Inc Ultrasonic Homogenizer* Available from: https://www.sonics.com/.
22. Fu, S.-Y., X.-Q. Feng, B. Lauke and Y.-W. Mai, *Effects of particle size, particle/matrix interface adhesion and particle loading on mechanical properties of particulate–polymer composites.* Composites Part B: Engineering, 2008. **39**(6): p. 933-961.
23. Dittanet, P. and R.A. Pearson, *Effect of silica nanoparticle size on toughening mechanisms of filled epoxy.* Polymer, 2012. **53**(9): p. 1890-1905.
24. Widom, B., *Random Sequential Addition of Hard Spheres to a Volume.* The Journal of Chemical Physics, 1966. **44**(10): p. 3888-3894.
25. Sasso, M., G. Palmieri, G. Chiappini and D. Amodio, *Characterization of hyperelastic rubber-like materials by biaxial and uniaxial stretching tests based on optical methods.* Polymer Testing, 2008. **27**(8): p. 995-1004.
26. Charlton, D.J., J. Yang and K.K. Teh, *A Review of Methods to Characterize Rubber Elastic Behavior for Use in Finite Element Analysis.* Rubber Chemistry and Technology, 1994. **67**(3): p. 481-503.
27. Yeoh, O.H., *Some benchmark problems for FEA from torsional behavior of rubber.* Rubber Chemistry and Technology, 2003. **76**(5): p. 1212-1227.
28. Mohan, C.V.R., J. Ramanathan, S. Kumar and A.V.S.S.K.S. Gupta, *Characterisation of materials used in flex bearings of large solid rocket motors.* Defence Science Journal, 2011. **61**(3): p. 264-269.

Table 1: Dynamic viscosity versus filler concentration

S.No	Filler Concentration (%)	Viscosity (cP)
1	0	6048
2	2	7545
3	4	8289
4	6	9960
5	8	14860
6	9	16900
7	10	25000
8	11	35700
9	12	79800

Table 2: Process parameters used to print the samples

Process Parameters	**Variables**		
Print Setting	Layers and Perimeters	*Layer height (mm)*	3.22
		First layer height (mm)	0.20
	Infill	*Fill density (%)*	40
	Speed (print moves)	*Perimeters (mm/s)*	20
		Infill (mm/s)	40
	Overall Time/Sample	*(min)*	10
Filament Setting	Filament	*diameter (mm)*	1
	Extrusion	*Extrusion multiplier*	0.0055

Table 3: Mechanical properties of 8%, 9% and 10% filler concentrations

Filler Concentration (%)	**Tensile Strength (MPa)**	**Strain at Break (%)**
8%	28	11
9%	22.2	5.6
10%	23.6	8.6

Table 4: Material constants for Yeoh's SEDF

C_{10} (MPa)	C_{20} (MPa)	C_{30} (MPa)	D_1	D_2	D_3
76.88	-1225.40	13201.63	6.002e-3	0	0

Table 5: Prony series coefficients

	G(i)	K(i)	Tau(i)
1	0.2950	0	23.90
2	0.4050	0	451.61

Figure 1: A schematic of the 5 axes photopolymer extrusion printer

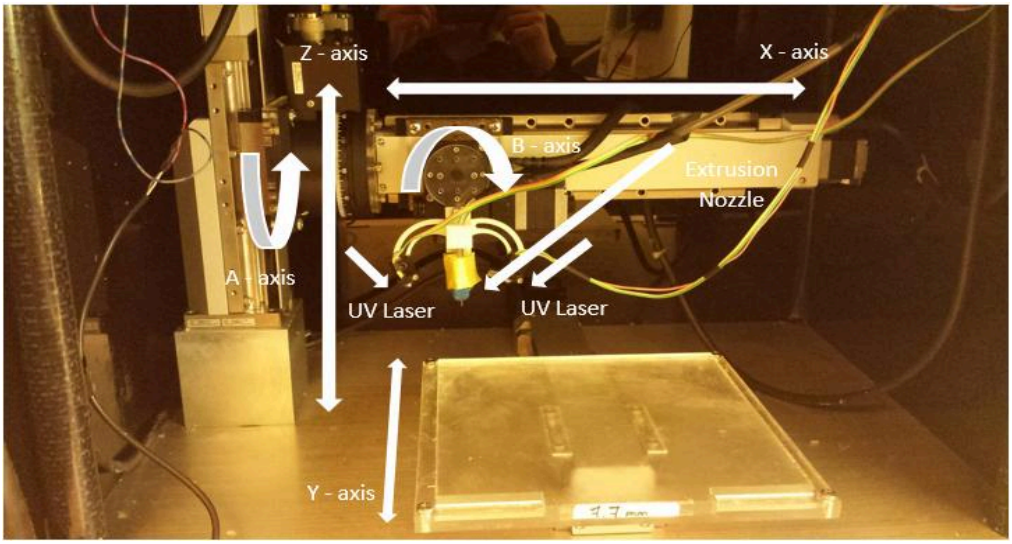

Figure 2: Close up view of the 5 axes PPE printer

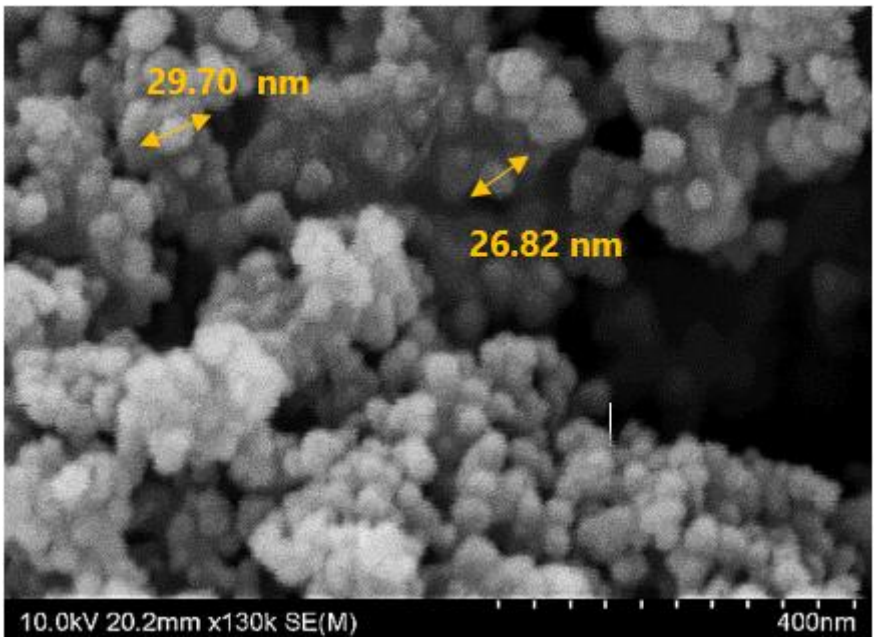

Figure 3: SEM of the silica nanoparticles

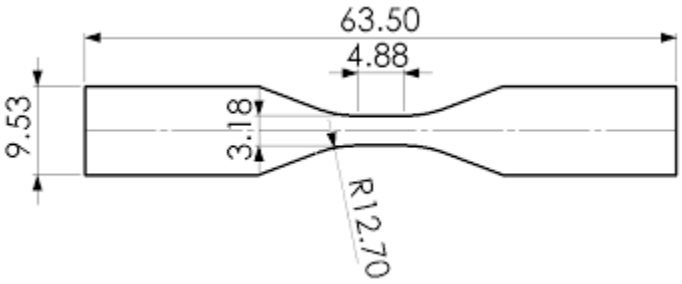

Figure 4: ASTM (D638) type V dog-bone specimen

Figure 5: ASTM D638 and printed specimen

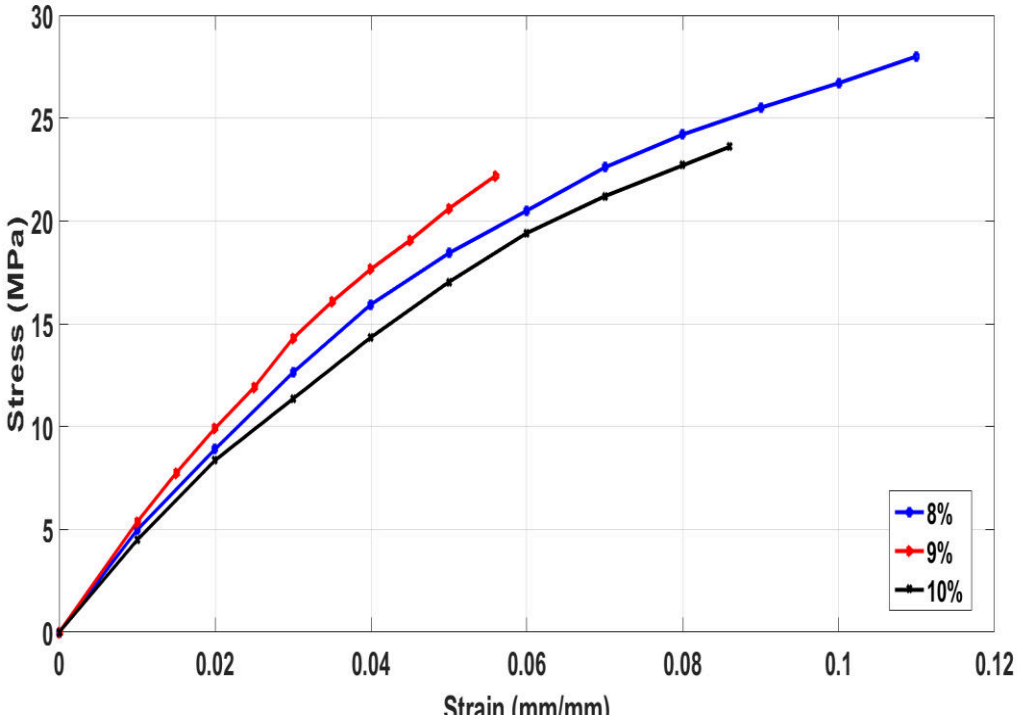

Figure 6: Stress-strain curve of 8%, 9% and 10% filler concentrations

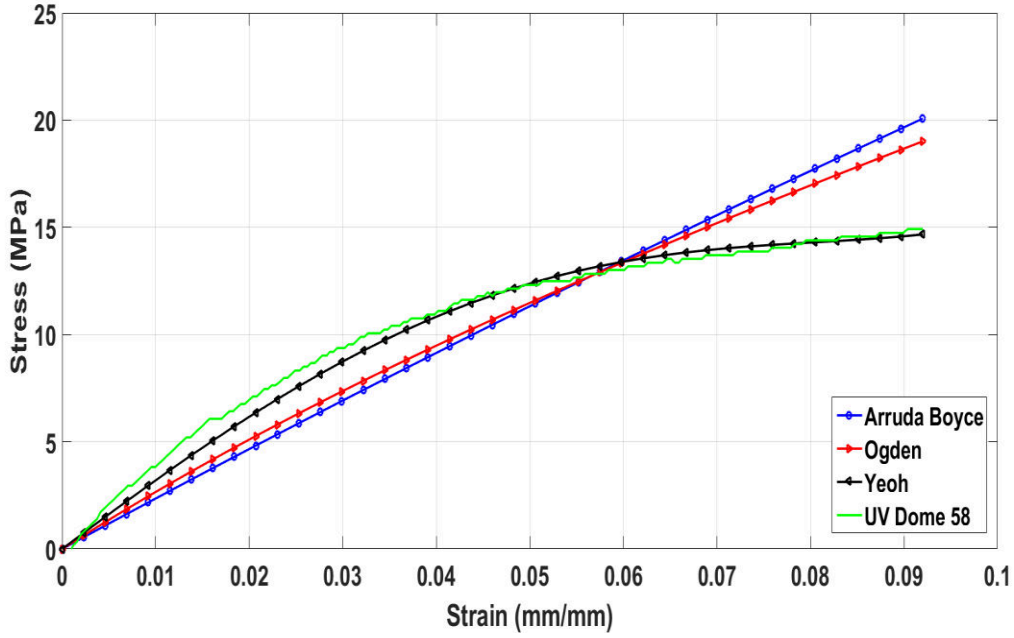

Figure 7: Curve fitting using different SEDF in ABAQUS

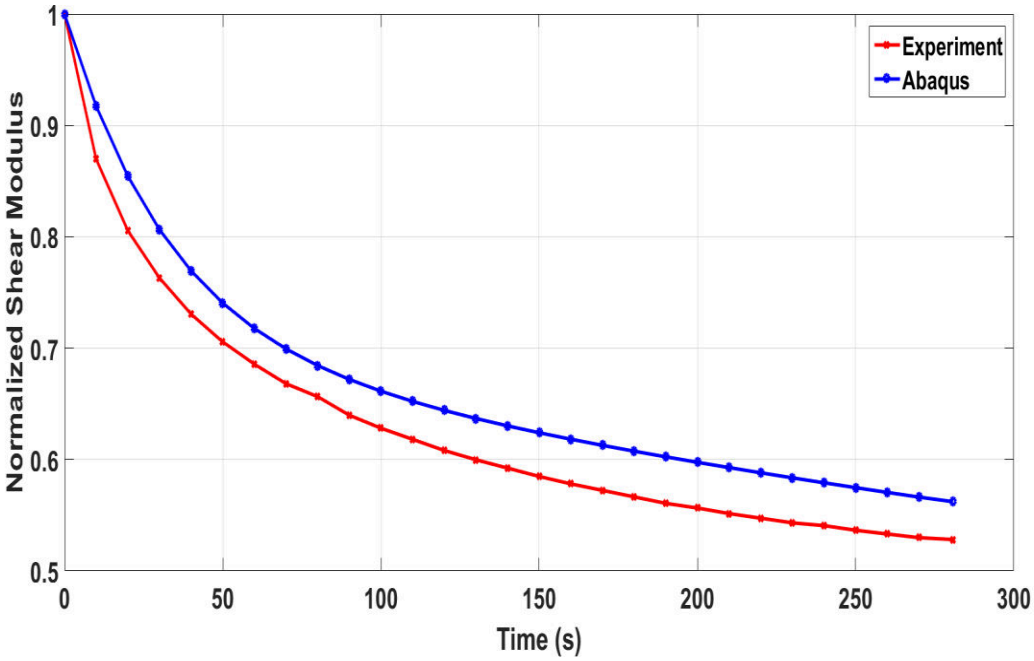

Figure 8: Normalized shear modulus vs Time

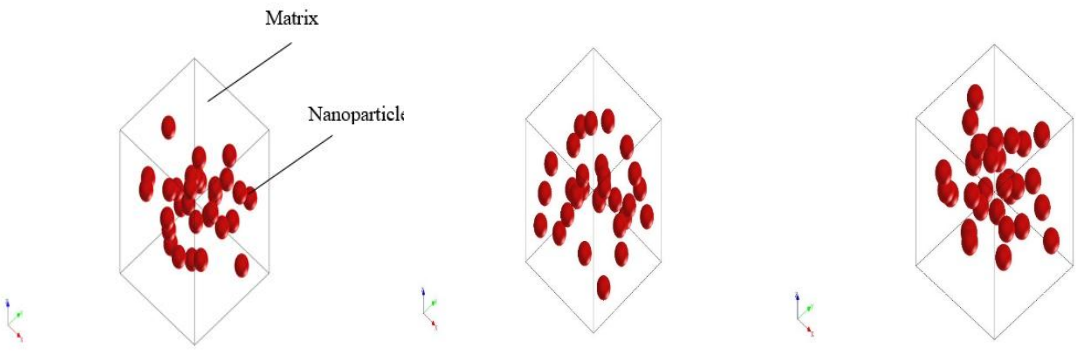

Figure 9 (a) RVE showing 8% filler concentration nanostructure (b) RVE showing 9% filler concentration nanostructure (c) RVE showing 10% filler concentration nanostructure

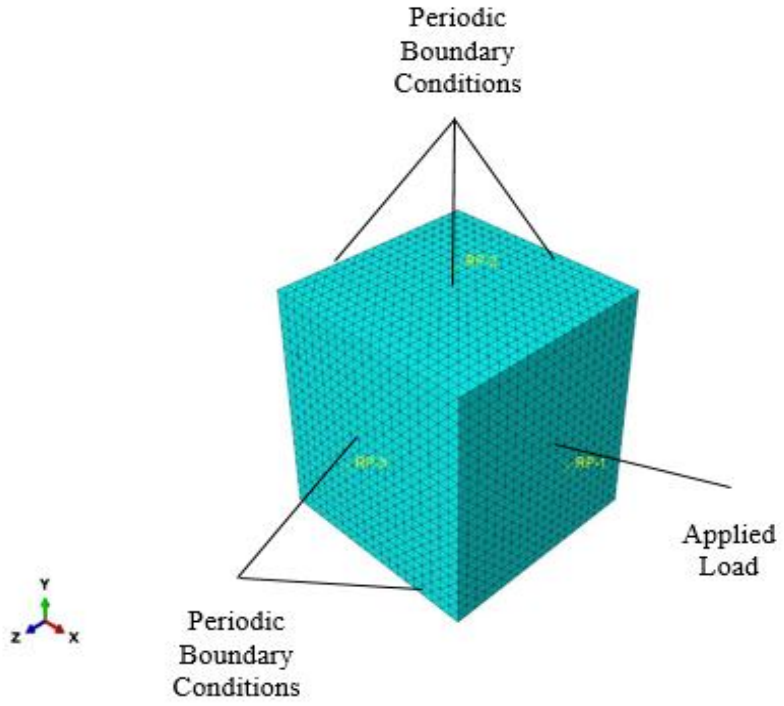

Figure 10: RVE showing periodic boundary conditions, applied load and mesh

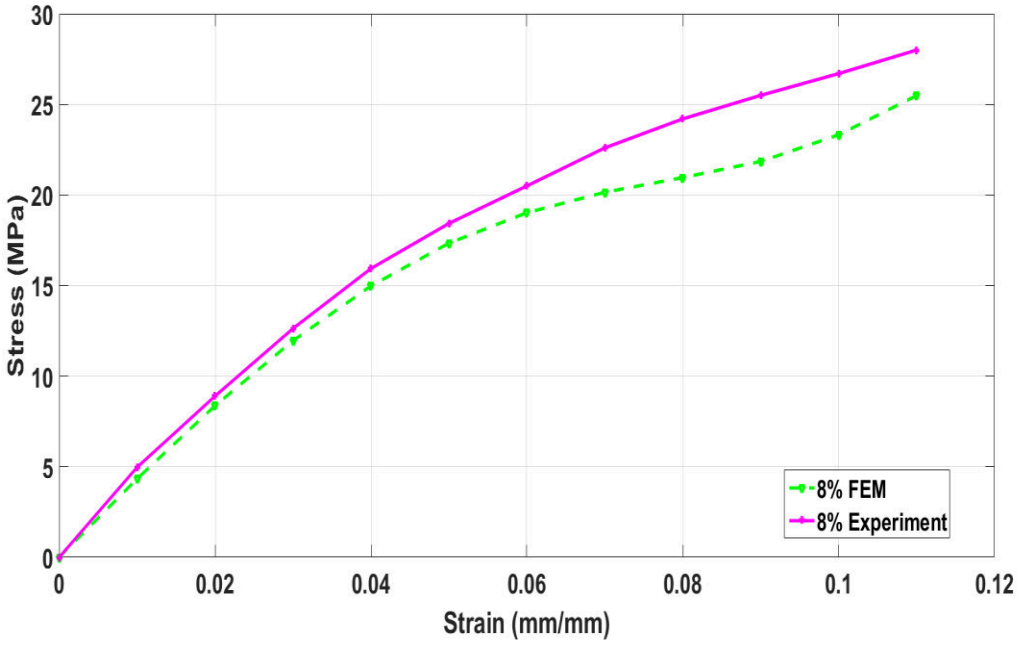

Figure 11: Comparison of stress-strain curve obtained from experiments and FEM for 8% filler concentration

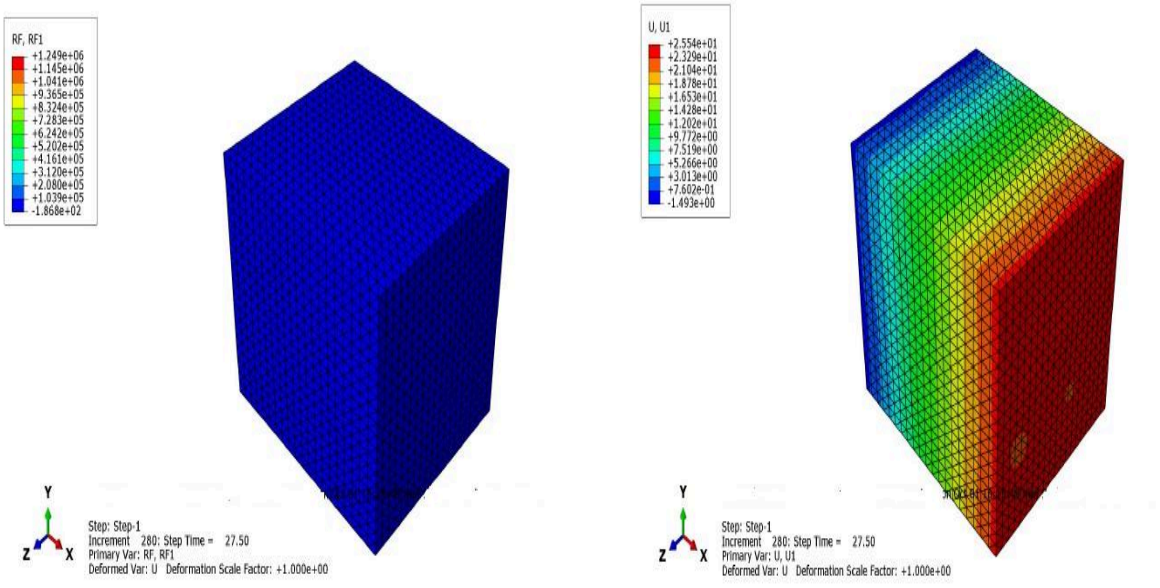

(a) (b)

Figure 12: Contour plot showing (a) reaction force and (b) displacement for 8% filler concentration

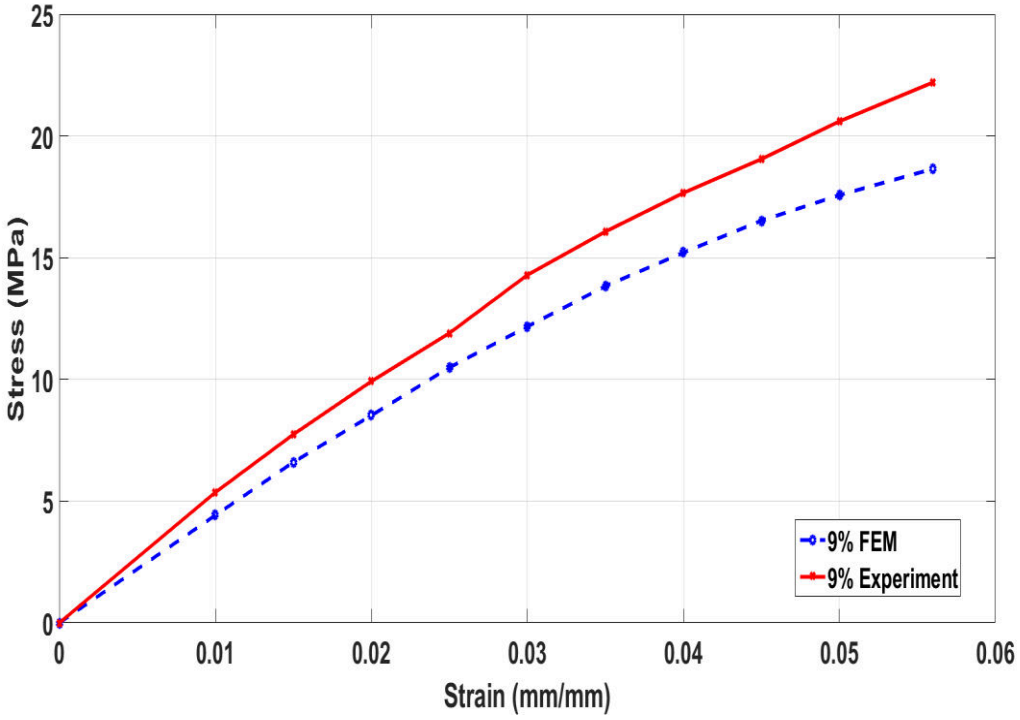

Figure 13: Comparison of stress-strain curves obtained from experiments and FEM for 9% filler concentration

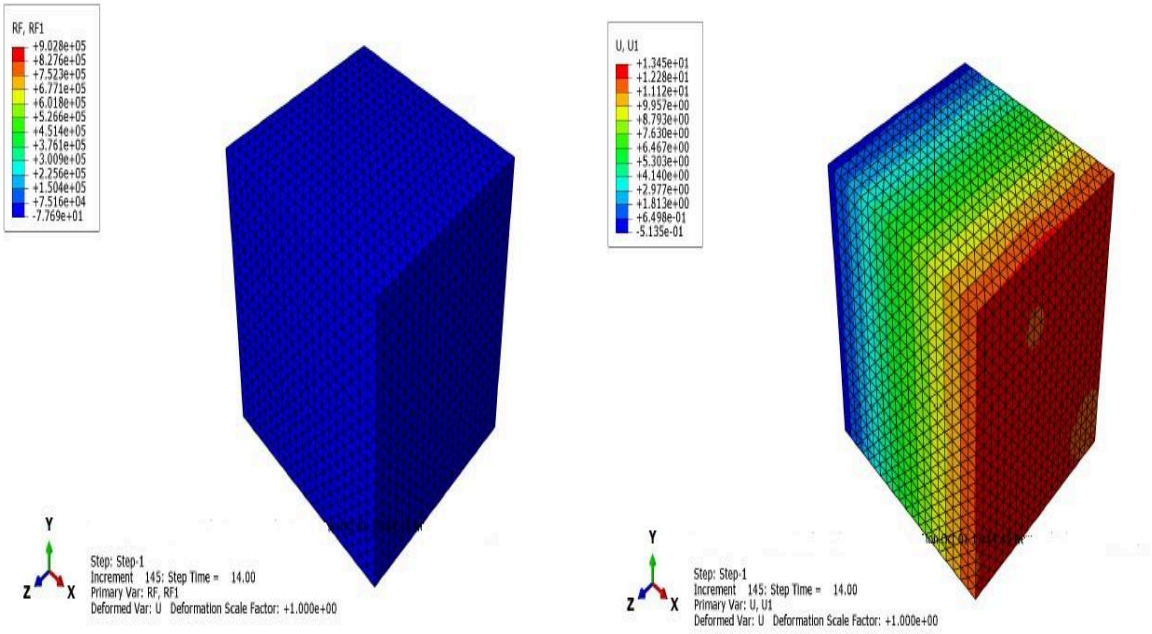

(a) (b)

Figure 14: Contour plot showing (a) reaction force and (b) displacement for 9% filler concentration

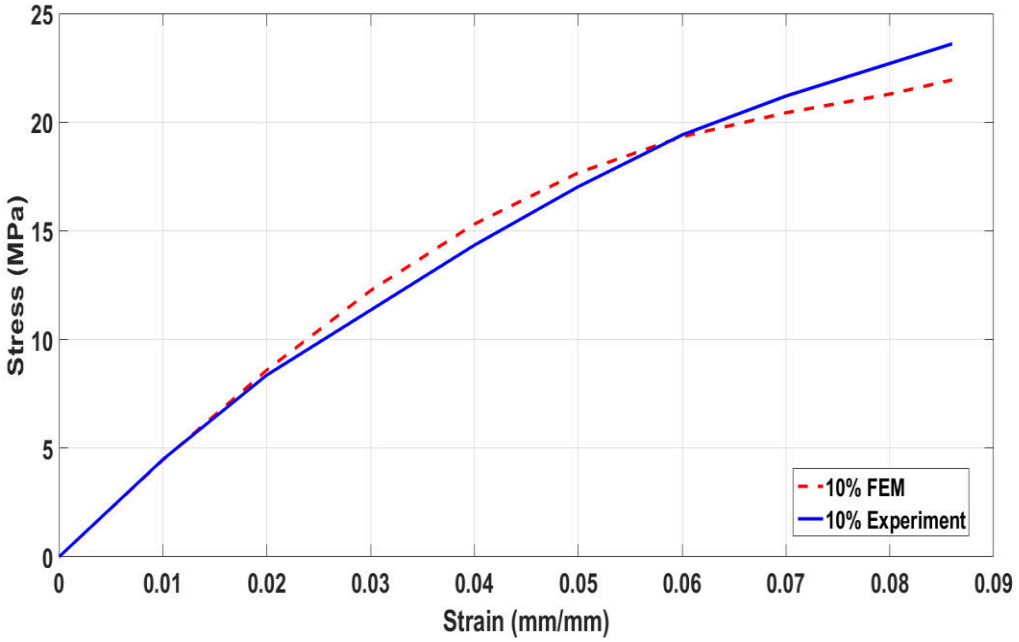

Figure 15: Comparison of stress-strain curve obtained from experiments and FEM for 10% filler concentration

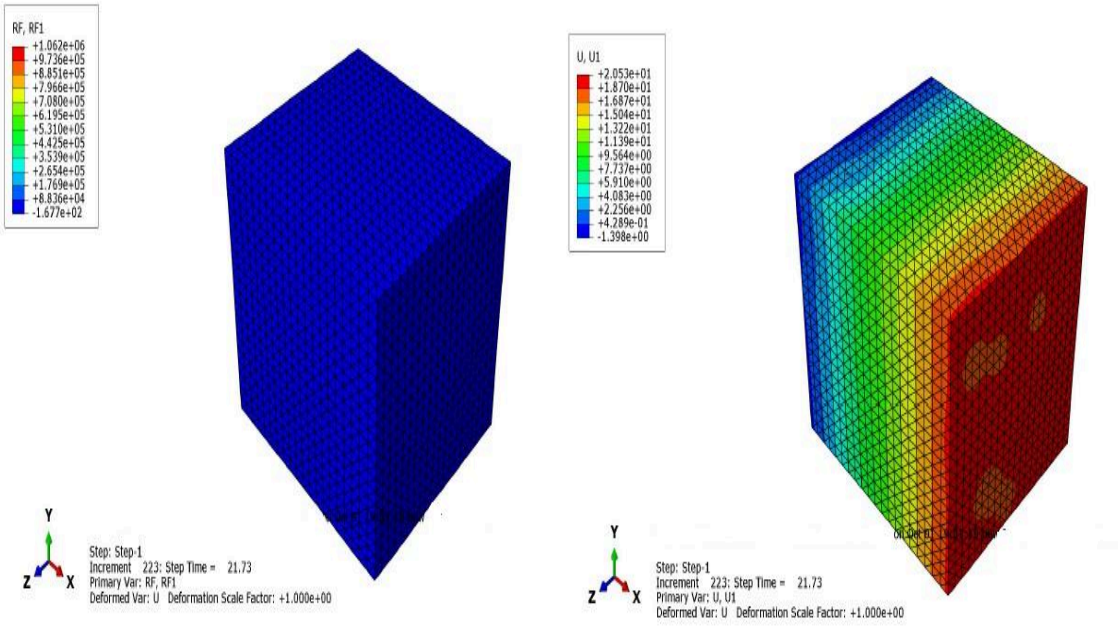

(a) (b)

Figure 16: Contour plot showing (a) reaction force and (b) displacement for 10% filler concentration

2019-09-03

Experimental and numerical study of the effect of silica filler on the tensile strength of a 3D-printed particulate nanocomposite

Asif, Muhammad Usman

Elsevier

Asif M, Ramezani M, Khan AK. (2019) Experimental and numerical study of the effect of silica filler on the tensile strength of a 3D-printed particulate nanocomposite. Comptes Rendus Mécanique, Volume 347, Issue 9, September 2019, pp. 615-625

https://doi.org/10.1016/j.crme.2019.07.003